SPECTROSCOPIC FACTOR FROM ^{6}Li(^{3}He,d)^{7}Be AND ASTROPHYSICAL FACTOR FOR ^{6}Li(p,γ)^{7}Be

N. Burtebayev[1], A. Amar[2], S.B. Sakuta[3], S.V. Artemov[4], Zh. Kerimkulov[1]
[1]*Institute of Nuclear Physics of National Nuclear Center, Almaty, Kazakhstan*
[2]*Kazakh National University, Almaty, Kazakhstan*
[3]*Russian Research Center "Kurchatov institute", Moscow, Russia*
[4]*Institute of Nuclear Physics, Tashkent, Uzbekistan*

Angular distributions of differential cross sections have been measured for elastic, inelastic scattering and the (^{3}He,*d*) reaction on ^{6}Li nucleus at the 34 MeV ^{3}He energy. Elastic scattering data at 34, 50, 60, and 72 MeV have been reanalyzed with optical model potentials taking into account elastic triton transfer mechanism and spectroscopic factor of ^{6}Li as t+^{3}He was re-extracted using Fresco program. Parameters for real part of potential have been also calculated microscopically with double-folding model. The differential cross sections for proton stripping to the ^{7}Be ground and first excited states have been analyzed by CRC methods at 34 MeV. The effect of triton exchange on proton transfer reaction ^{6}Li(^{3}He,*d*)^{7}Be for both ground and excited state is discussed. Spectroscopic factors for ^{7}Be as p^{6}Li configuration have been obtained from the experimental data. New measurements of the ^{6}Li(p,γ)^{7}Be reaction γ-ray angular distributions have been done at beam energies of $E_{p,\,lab.}$ = 387, 690, 984 and 1283 keV for the γ-ray transitions to the ground and first excited ($1/2^-$, 429 keV) states in ^{7}Be. Our calculations of the cross section of the ^{6}Li (p, γ)^{7}Be reaction was carried within the framework of the direct capture in the potential model using Fresco program. We extracted both of spectroscopic factors of ^{7}Be and astrophysical factor ^{6}Li+p→^{7}Be+γ from experimental data.

Introduction

Solving the scattering or reaction problem with the Schrödinger equation requires knowledge of the interaction potential between the two colliding nuclei. Unlike the Coulomb potential, the nuclear one is less known, especially at small distances of the interacting nuclei. From the phenomenological studies, it got clear that the major part of the nuclear interaction potential can be approximated by a Woods-Saxon form which gives a simple analytic expression, parameterized explicitly by the depth, the radius, and diffuseness of the potential well. In practice the optical model potential (OMP) is in use [1]. The OMPs are widely employed to generate the distorted waves used to analyze the cross section of many reactions, and these analyses have proved to be powerful tool to extract nuclear structure information. But the applicability of the optical model and distorted wave Born approximation (DWBA) for light nuclei in its simple form is somewhat dubious because the number of target nucleons is small. Moreover, cluster effects might become important in the elastic scattering and reactions. Although the optical model and DWBA theory are not expected to work well for the nuclei with A=6 and 7, a study of the transfer reactions on these light targets is attractive as many properties of these light systems have been calculated in detail. It is known that by the interaction of the complex particles with light nuclei there is often observed the specific effect called as an anomalous large-angle scattering (ALAS), which is impossible to explain in the framework of the standard optical model. The nature of this phenomenon can be caused by different reasons, but in certain cases when the targets are ^{6}Li and ^{7}Li, having the pronounced (α+*d*) and (α+*t*) cluster structure increase in the cross section at large angle is almost entirely connected with the transfer exchange mechanism, physically undistinguished from potential scattering [2].

The results of DWBA analysis of the transfer cross sections are typically highly sensitive to the optical potential parameters. The calculated angular distribution of the nucleon transfer reaction can vary significantly even through the used OMPs fit rather well the elastic scattering in the entrance and exit reaction channels. Moreover, different optical potential parameterizations can provide spectroscopic factors (SFs) different up to factor 2. Consequently, it is very important to pin these down as much as possible. Whether there is adequate elastic data to determine the optical

parameters or not, it is important to evaluate the uncertainty in the obtained SFs caused by U_i and U_f [3]. The ability to extract the SF in transfer reaction depends on whether the reaction mostly takes place in the surface, in the periphery, or more in the interior of the nucleus. It is common to obtain the empirical SF S^{exp} by direct comparison with the data, fitting up to the first maximum of the angular distribution for the projectile-like outgoing particle. As one moves to larger angles, the DWBA is no longer expected to provide reasonable results, even for the angular distribution of the cross section (this true for transfer but also inelastic scattering, charge exchange, etc.). If only very forward angle are used, by contract, it may be that the transfer is completely peripheral and thus no longer sensitive to the interior. In such case the result of analysis depends weaker on the ambiguities of OMP [3]. The OMPs are widely employed to generate the distorted waves used to analyze the cross section of many reactions, and these analyses have proved to be powerful tool to extract nuclear structure information [4]. Reactions at astrophysical energies are complicated by the fact that the matter-interaction energy in stars is very low, ranging between a few tenths of a keV unit and a few tens of keV units. With a few exceptions, it is next to impossible under laboratory conditions to measure directly, at such energies, nuclear-reaction cross sections, which are necessary for astrophysical calculations. Usually, cross sections are measured at higher energies, whereupon the results are extrapolated to the energy region of interest for nuclear astrophysics. As a rule, however, the measurements actually performed cover only the region of rather high energies from about 0.2 to 1 MeV. In view of this, an extrapolation of such experimental data to the astrophysical region is not always justified. As a result, only theoretical predictions can compensate in many cases for missing experimental information about the properties of astrophysical thermonuclear reactions. Under such conditions, resort to realistic models that are rather simple in practical applications, such as the potential cluster model (PCM), seems quite justified. Usually, the results of calculations performed on the basis of model concepts are contrasted against available low-energy experimental data, and approaches leading to the best agreement with these data are selected by using the results of this comparison. After that, calculations in the region of astrophysical energies are performed within the chosen conceptual framework. One can consider the results obtained in this way (for example, those concerning astrophysical *S* factors) as more realistic estimates of respective quantities than the extrapolation of experimental data, since the theoretical models used have, as a rule, quite a sound microscopic basis [5]. Radiative capture of nucleons at energies of astrophysics interest is one of the most important processes for nucleosynthesis. The nucleon capture can occur either by a compound nucleus reaction or by direct process. The compound reaction cross sections are usually small, especially for light nuclei. The direct capture proceeds either via the formation of a single-particle resonance or non-resonant capture process. Unlike ^{7}Li and ^{6}Li to be formed at very low level in Big Bang nucleosynthesis, with abundance ratio Li/H = 10^{-14}. Whereas most elements are produced by stellar nucleosynthesis, lithium is mainly destroyed in stellar interiors by thermonuclear reactions with protons. In fact, ^{6}Li is rapidly consumed at stellar temperature 2×10^6 K. The low energy capture reaction ^{6}Li(p,γ)^{7}Be plays an important role in the consumption of ^{6}Li and formation of ^{7}Be [6].

The S-factor of this reaction is dominated by captures to the ground state and first excited state of ^{7}Be. However, the number of studies devoted to measuring the total cross section for this reaction and to experimentally determining its astrophysical *S* factor in the region of low energies is comparatively small [7].The ^{6}Li(p,γ)^{7}Be reaction has been experimentally studied by Switkowski et al. [8] at low energies down to 200keV. A theoretical extrapolation has been performed by Barker [9] within potential model, based on simultaneous fit of ^{6}Li(n,γ)^{7}Li and ^{6}Li(p,γ)^{7}Be cross sections. K. Arai et al. [10] used a four cluster microscopic model to investigate low-energy ^{6}Li+p and ^{6}Li+n reactions.

The ^{6}Li(p,γ)^{7}Be reaction S-factor is in [10] good agreement with the available experimental data. Knowledge of the rate of change of the *S* factor with energy at very low energies is needed to perform a reliable extrapolation. Although this is frequently determined by the use of a direct

capture-model calculation, there are cases when this does not suffice. Low-energy resonances or sub-threshold states can affect the extrapolation. In [11] the results of a measurement of the slope of the astrophysical *S* factor for the ^{6}Li(p,γ)^{7}Be reaction are reported, and a new mechanism is introduced to explain the observed slope. Cecil *et al.* [12] measured the branching ratio of ^{6}Li(p,γ_0)^{7}Be and ^{6}Li(p,γ_1)^{7}Be with respect to ^{6}Li(p, α)^{3}He from 45 to 170 keV and deduced the *S* factors for ^{6}Li(p,γ_0)^{7}Be and ^{6}Li(p,γ_1)^{7}Be as a function of energy. Their results gave a positive slope for the *S* factor. Switkowski *et al.* [8] measured the ^{6}Li(p,γ)^{7}Be cross section from 160 to 1150 keV. Their data points are all at energies above the present data set and show an *S* factor that increases with increasing energy. Barker's analysis [9] of the data of Switkowski *et al.* does have a negative *S*-factor slope for ^{6}Li(p,γ_0)^{7}Be and ^{6}Li(p,γ_1)^{7}Be at energies below the range of the data. The present measurements were undertaken to examine this discrepancy in the previous measurements of Cecil *et al.* and Switkowski *et al.*

The purpose of this work is a search of the correct OMP for ^{6}Li+^{3}He channel taking into account besides the "potential" scattering also coupling with the inelastic channel as well as the mechanism of triton pick-up. The next aim is to obtain the SFs of ^{7}Be→^{6}Li+*p* bound configurations from the experimental differential cross sections of the ^{6}Li(^{3}He,*d*)^{7}Be reaction for afterwards calculation of the contribution of direct proton capture to astrophysical *S*-factor ^{6}Li+*p*→^{7}Be+γ.

Experimental data

a) ^{6}Li (p, p)^{6}Li

Measurements of elastic scattering of protons on ^{6}Li nuclei at low energy region were carried out with using the extracted beam from UKP-2-1 accelerator of the Institute of Nuclear Physics (National Nuclear Center, Republic of Kazakhstan, Almaty, Kazakhstan) in the angular range 30-170˚. The proton energy varied in the range 400 – 1150 keV. The beam intensity was 50 – 150 nA. Scattered particles were detected using surface-barrier silicon counters. Analysis and experimental set up was mentioned in [13,14].

b) Elastic scattering of ^{3}He on ^{6}Li nuclei and ^{6}Li(^{3}He,*d*)^{7}Be reaction at 34 MeV

Measurements of the elastic scattering of ^{3}He on ^{6}Li nuclei and ^{6}Li(^{3}He,*d*)^{7}Be reaction at 34 MeV have been carried out using the extracted beam of cyclotron U-150M of the Institute of Nuclear Physics (National Nuclear Center, Republic of Kazakhstan, Almaty). Differential cross sections have been measured in the angular range 6□-72□ for elastic scattering and ^{6}Li(^{3}He,*d*)^{7}Be reaction with steps 2□-4□. Lithium targets were films deposited on the thin backing of Al_2O_3 by the vacuum evaporation method. Thicknesses of films in interval 200-300 μg/cm^2 were measured with the accuracy ~ 5%. The special vacuum lock chamber was used for transportation of the targets from evaporating system to the reaction chamber.

The energy spectra of the resulting particles were measured using two Δ*E*-*E* telescopes of semiconductor detectors. The absolute errors of the differential cross sections not exceed 10%. A typical deuteron spectrum from the ^{6}Li(^{3}He,*d*)^{7}Be reaction is shown in Fig. 1.

c) ^{6}Li(p, gamma)^{7}Be

In experiment for determination of cross-sections of the ^{6}Li(p,γ)^{7}Be reaction, it was used special manufactured chamber with indium vacuum seals, systems of fine adjustment and visual control of the form of proton beam and its position on the target during all measurements, with the possibility of precise placement of the target exactly into the chamber center and of its additional equipment by nitrogen trap and additional magneto-discharge pump. The new reaction chamber was connected to the output flange of the central scattering chamber, completed by turbo-molecular and magneto-discharge pumps and by the system of nitrogen traps. The typical pressure in the reaction chamber was $1.5\cdot10^{-6}$ mm Hg, and the experimental error, stipulated by the formation of carbon deposit on the target during the measurement, was negligible. The measurements of angular

distributions of gamma-quanta from the $^{6}Li(p,\gamma)^{7}Be$ for transitions were for the ground state and first excited state (429 keV) of the ^{7}Be at energies of incident protons of 387, 690, 984 and 1283 keV. Currents of the protons beam, incident upon targets, were equal to (5-8) μA. During the measurement of the integral current the collected charge was from 0.05 to 0.25 Coulomb. Targets were placed in the chamber for the study of (p,γ) reactions.

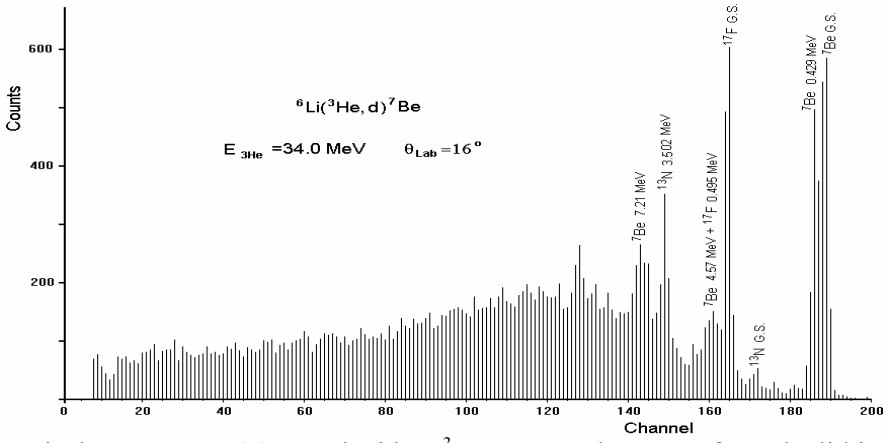

Fig. 1. Typical spectrum at 34 MeV incident ^{3}He energy: deuterons from the lithium target

In order to prevent the overload of the electronics, caused by the powerful background line with the energy of E_γ=478 keV, connected with progresses, $^{7}Li(p,p\gamma)^{7}Li$ and $^{7}Be \rightarrow {}^{7}Li^{*}+\beta^{+}+\nu \rightarrow {}^{7}Li+478$ keV, between the detector and the reaction region there was put the flat lead plate of the 1 cm-thickness. Besides, the intensity of the line with E_γ=478 keV decreases by a factor of about 5, whereas the intensity of lines from the $^{6}Li(p,\gamma)^{7}Be$ reaction (with E_γ=6000 keV) decreases only by several per cent. Fig.2. is an example of the γ-spectrum, obtained at $E_{p,lab}$=984 keV, $\theta_{\gamma,lab.}=0^{\circ}$. In figure there are well seen background lines, 1461 keV (^{40}K), and the annihilation line with E_γ=511 keV. Well-known energies of γ-transitions for these lines allowed to control the energy calibration. Peaks of the total absorption and peaks of unitary and double leakages for γ-transitions onto the ground and the first excited state of the ^{7}Be shown in Figure 2, with the use of the HpGe – detector (GEM20P) of the 111cm^{3} –volume, placed in 6 cm from the reaction region.

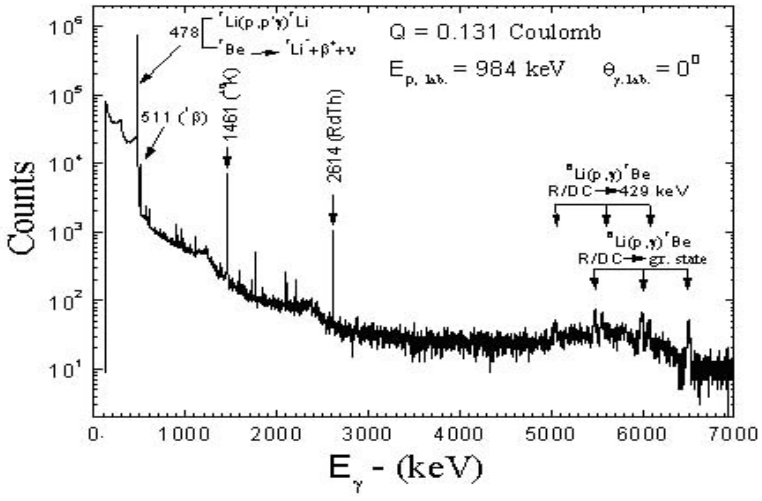

Fig. 2. An example of the γ-spectrum of the $^{6}Li(p,\gamma)^{7}Be$ reaction

Results and discussions

a) Phenomenological Elastic Scattering of protons on ^{6}Li

The analysis of protons data, carried out at wide energy range, had shown that for ^{6}Li nuclei, the most suitable parameters values are r_0=1.05fm, r_c=1.3fm, r_D=1.923fm, a_s=0.20fm and r_s=1.20 fm.

Table 1. The phenomenological optical parameters for protons scattering on Lithium nuclei

E_p, MeV	V_0, MeV	r_0, fm	a_0, fm	W_D,MeV	r_D, fm	a_D, fm	V_S, MeV	r_s, fm	a_S, fm	J_R, MeVfm^3	J_w, MeVfm^3
0.746	59	1.05	0.85	0.300	1.923	0.575	9.30	1.077	0.66	490	20.47
0.975	57.2	1.050	0.67	0.355	1.923	0.650	9.30	1.020	0.200	475	22.19
1.136	54	1.05	0.52	0.355	1.923	0.57	9.30	1.020	0.200	454	22.19

In the analogous approach with the use of measured on the elastic scattering there are determined parameters of the potential of protons scattering on ^{6}Li nuclei from the analysis of these data on the optical model. Obtained parameters of optical potentials of the interaction are presented in Table 1. The relations between $V(W_D)$ versus E_p are linear. The strength parameters can be represented by: $V_0 = 56.10 - 0.61E_p$, $W_D = -0.66 + 0.46E_p$, respectively.

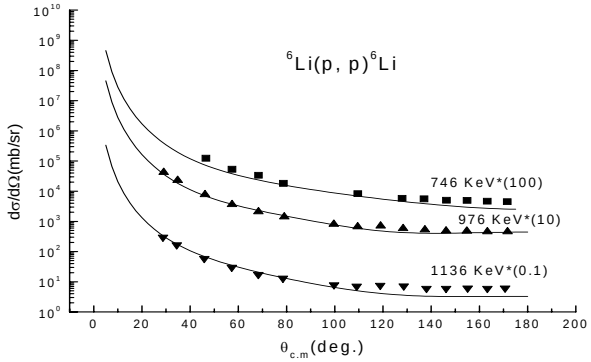

Fig. 3. The comparison between calculated and experimental angular distribution of protons scattered from ^{6}Li at low energies where dots represent experimental data and lines represent the calculated values

b) Analysis of the ^{6}Li(^{3}He,^{3}He)^{6}Li, ^{6}Li(^{3}He, ^{6}Li)^{3}He

Elastic scattering of ^{3}He on ^{6}Li at the energies 34, 50, 60 and 72 MeV has been reanalyzed using FRESCO [15] program. The ground state of ^{6}Li is dominated by the two overlapping configurations: α+d and ^{3}He+t. In the oscillator picture, the anti-symmetrized wave functions for lowest T = 0 ^{6}Li states expressed as α+d and ^{3}He+t are mathematically equivalent. This cluster aspect plays an important role in nuclear reactions and its effects can be seen even in the elastic scattering of d, ^{3}He and α particles from ^{6}Li. The phenomenological analysis of Bragin et al. is suggested [16] that ^{3}He+^{6}Li elastic scattering at 34, 50, 60, and 72 MeV can be explained if a triton is exchanged between ^{3}He projectile and ^{3}He core of ^{6}Li. A coherent sum between the "potential" elastic scattering and elastic triton transfer generated a back angle rise in cross section. The energy dependence of extracted SFs for ^{6}Li={^{3}He+t}were attributed to the inaccuracy of the knowledge of the real part of the optical potential and it was suggested that the inclusion of other reaction mechanisms could change the values of SFs [17]. A choice of optical parameters is so important because wrong estimation of OMP used in elastic part would lead to the use of wrong SF to match the back angle rise. In [17] they calculated the cross section $d\sigma/d\Omega$ using the relation

$$d\sigma / d\Omega = \frac{1}{4}\left|f_{el}(\theta) + Sf_{tr}(\pi - \theta)\right|^2 + \frac{3}{4}\left|f_{el}(\theta) - Sf_{tr}(\pi - \theta)\right|^2 , \quad (1)$$

where $f_{el}(\theta)$ is the amplitude of the potential scattering, $f_{tr}(\pi-\theta)$ is the amplitude of elastic transfer and S is SF for ^{6}Li=$\{^3$He+$t\}$. Because of large Q-value of ^{6}Li$\rightarrow^3$He+t (Q=-15.796 MeV) break up, the triton cluster exchange model is expected to be more valid at a higher incident energy. We reanalyzed the data at 34, 50, 60 and 72 MeV using Fresco program. Simmonds et al. [18] used in their analysis of ^{6}Li$\rightarrow^3$He+t bound state wave function, they took the geometry parameters of Wood-Saxon potential for bound state as r_s = 0.85 *fm*, a_s = 0.65 *fm* and r_C= 0.85 *fm*, where $R=r_x A^{1/3}$ which is more suitable in our analysis than the standard form (r_s=1.25 *fm* and a_s=0.65 *fm* and r_C=1.3 *fm*. We tested some sets of OMP at the analysis of ^{6}Li(^{3}He,^{3}He)^{6}Li elastic scattering data which were taken from the literature data as well as from the folding model calculation. To compare our fitting with the semi-microscopic analysis of T. Sinha *et al.* [17] we repeated the calculations of them with another form of bound state wave function and OMP parameter sets 4 and 10-15 in table 2 at both the entrance and exit channels using CRC calculations. The depth of real potential was deeper to 113MeV to give suitable analysis at 50 MeV incident energy of ^{3}He and to 137 MeV in case of 60 MeV of incident energy of ^{3}He . In 72 MeV deeper real potential needed, it was about 140 MeV. For the imaginary part we used the imaginary parameters from the semi-microscopic analysis from Sinha et al. For 50, 60, 70 MeV an adjustment for imaginary potential was needed and it is shown in table 2. A good fit was obtained by changing the imaginary potential for energies under considerations. The standard form of bound state was used, but it was not the ideal form for analysis so, we used another form of bound state. Simmonds et al. [18] used in their analysis of ^{6}Li$\rightarrow$ ^{3}He+t bound state wave function, they take took the parameters for bound state potential as r_s=0.85 and a_s=0.65 and r_c=0.85*fm* where R=$r_x A^{1/3}$. We made some modifications in this form to become as $R = r_x(A_p^{\frac{1}{3}} + A_t^{\frac{1}{3}})$, and it gave us a suitable analysis as shown in Figures 4 (b, d, e, f).

The folding model has been used for years to calculate the nucleon-nucleus optical potential. The real part of the OMP for the nucleus–nucleus elastic scattering is given for the double folding model, in the following form:

$$V_F(r) = \int dr_p \int dr_t \rho_p(r_p)\rho_t(r_t)v(r_{pt}), \tag{2}$$

where ρ_p is the projectile matter density distribution, ρ_t is the matter distribution of the target and r_{pt} = $r + r_t$ - r_p. A popular choice for the effective NN interaction has been one of the M3Y interactions. In the present calculation the effective NN-interaction is taken according to the form of M3Y-interaction:

$$v(r) = 7999\,\frac{\exp(-4r)}{4r} - 2134\,\frac{\exp(-2.5r)}{2.5r} - 276\left(1 - \frac{0.005\,E}{A_p}\right)\delta(R) \tag{3}$$

The density distribution of ^{3}He was taken to be Gaussian form [19]:

$$\rho_p(r) = c\exp(-\alpha r^2), \tag{4}$$

where c = 0.20816 fm^{-3} and α = 0.53047 fm^{-2}, these parameters correspond to a root-mean square (RMS) radius of ^{3}He of 1.68 fm. The nuclear density distribution of ^{6}Li was taken according to [20]:

$$\rho_t = \frac{1}{8\pi^{3/2}}\left(\frac{1}{a^2}\exp\left(-\frac{r^2}{4a^2}\right) - \frac{c^2\left(6b^2 - r^2\right)}{4b^7}\exp\left(-\frac{r^2}{4b^2}\right)\right) \tag{4'}$$

where a, b, and c are constants: a^2 = 0.87 fm^2, b^2 =1.7 fm^2 and c^2 = 0.205 fm^2. The real potential $V_F(r)$ is obtained by integrating an effective nucleon-nucleon interaction over the density distributions of the two colliding nuclei. The real folded potential $V_F(r)$ was calculated using DFPOT [21] we used the potential:

$$U(r) = - NV_F(r) - iW(r) + V_C \tag{5}$$

The imaginary potential have the form mentioned in the ref. [18] which is used as starting potential. Normalization factor (N) and imaginary potential parameters have been changed to obtain the best fit of the data. The selected OMPs as well as potential used at the analysis of the (^{3}He,d) reaction

are presented in Table 2. Final folding potential parameters are shown in Table 2 with N=0.84 mentioned as DF P.W. (Double Folding, Present Work) and P.W. (column 13).
The analyses made by us for SFs for ^{6}Li=$\{^{3}$He+$t\}$have advantage that the calculations agree well with experimental data. T. Sinha et al. [17] to reduce the back angle rise of their calculations SF=0.45 for ^{6}Li=$\{^{3}$He+$t\}$ at 34, 50, 60 and 72 MeV was needed. A relatively better fit was obtained in [17] when they used energy dependent renormalization N_R and fixed spectroscopic factor 0.39 in their calculations (see ref. [17]). In [17] they extracted the spectroscopic factor of the configuration ^{6}Li=$\{^{3}$He+$t\}$and it was 0.21. The analyses made before were so poor especially in [17] at energies 34, and 50 MeV, where in our work there is coincidence between experimental and theoretical calculations (see fig. 4 b, d, e, and f). SFs calculated at energies 34, 50, 60, and 72 agree with theoretical [8] which was 0.58. SFs for triton transfer with elastic scattering at 50, 60, and 72 MeV are 0.579, 0.341 and 0.435 respectively. The values of spectroscopic factors and potentials used in this analysis were used in CRC in proton transfer reaction ^{6}Li(^{3}He,d)^{7}Be in the last section. OMPs for ^{7}Li+d mentioned in [22] were taken as exit channel depending on the mirror effect between ^{7}Be and ^{7}Li and it was modified as shown in table 2.

Table 2. Optical model potentials for DWBA calculations of ^{3}He scattering on the nucleus ^{6}Li and the reaction ^{6}Li(^{3}He,d)^{7}Be. In the 1-st column are the assumed here names of OMPs; in the 2-nd column are the projectile energies for that the parameters were found; in the 6-th column the letter "V" means the volume Woods-Saxon form and the letter "D" means the surface (derivative) form of the imaginary part of OMP. P. W. means our calculations.

OMP name	$E_{lab.}$ MeV	V MeV	r_V *fm*	a_V *fm*	W MeV	r_W *fm*	a_W *fm*	V_{so} MeV	r_{so} *fm*	a_{so} *fm*	r_C *fm*	Ref
1	2	3	4	5	6	7	8	9	10	11	12	13
^{6}Li + ^{3}He												
0(1)	18.0	65.5	1.30	0.75	70.4 V	1.30	0.41	6.0	1.20	0.70	1.3	p.w.
1(1)	33.3	100.8	1.25	0.75	10.0 V	1.20	0.780	1.15	1.05	0.384	1.3	p.w.
2(1)	14.7	153.4	1.18	0.489	3.45 V	2.97	0.489				1.3	23
3(1)	33.3	171.0	1.106	0.685	17.0 V	1.388	0.591	1.72	1.363	0.180	1.3	24
4(1)	34.0	100.1	1.14	0.810	16.2D	1.12	0.854	1.15	1.05	0.384	1.3	25
4(1')	34.0	119.1	1.14	0.740	18.68D	1.20	0.728	1.15	1.05	0.384	1.3	p.w.
5(1)	18.0	140.0	1.20	0.83	30.0 V	1.93	0.42	6.0	1.20	0.70	1.3	26
6(1)	34.0	120.8	1.15	0.81	20.21 V	1.25	0.64	15.93	1.25	0.64	1.3	27
7(1)	34.0	122.30	1.15	0.70	23.64 V	0.88	0.80				1.3	DF-P.W
8(1)	34.0	118.30	1.30	0.82	38.5V	1.31	0.84	35.0	1.31	0.84	1.24	28
9(1)	34.0	118.30	1.30	0.82	38.5V	1.31	0.84	8.75	1.31	0.84	1.24	28
10(1)	50.0	113.8	1.15	0.748	22.45D	1.23	0.80					P. W.
11(1)	50.0	107.33	1.12	0.99	26.45D	1.23	0.80					P. W.
12(1)	60.0	110.0	1.15	0.755	22.5D	1.22	0.80					P.W.
13(1)	60.0	95.95	1.12	0.755	30.67	1.25	0.57					P. W.
14(1)	72.0	110.72	1.12	0.90	16.50	1.46	0.87					P. W.
15(1)	72.0	140.44	1.15	0.973	6.672	1.28	0.59					P. W.
^{7}Be + d												
0(2)	18	100.0*)	1.35	0.72	12.9D	1.94	0.30	8.0	0.86	0.25	1.3	22
1(2)	18	118.0	1.0	0.94	6.87D	1.98	0.59	8.5	1.0	0.94	1.3	26
2(2)	28	81.1	1.15	0.81	8.61D	1.34	0.873	6.0	1.15	0.81	1.15	23
3(2)	30	90.0	1.150	0.810	8.61 D	1.340	0.873	6.00	1.15	0.810	1.25	24
4(2)	30	90.0	1.150	0.810	12.61 D	1.340	0.873	6.00	1.15	0.810	1.25	24
5(2)	15.8	134.9	0.817	1.045	11.1 D	2.078	0.522	10.44	0.817	1.045	1.3	23
6(2)	27.7	74.03	1.239	0.736	11.67 D	1.239	0.736	10.44	0.817	1.045	1.24	23

*) – The value was corrected by [A. Amar et al. World Acad. Sci., Engineering&Techn, 74 (2011) 270]

Figures 4 (b, d, e, f) show the best fit for the elastic scattering of ^{3}He on ^{6}Li at the energies of 34, 50, 60 and 72 MeV for triton exchange with the elastic scattering. Inelastic scattering at $E_{^{3}He}$=34 MeV has been analyzed where intrinsic quadrupole moment was (-0.818 mb) and B(E2)= 25.6±2.0 e^2 fm^4 [29] as shown in fig. 4c.

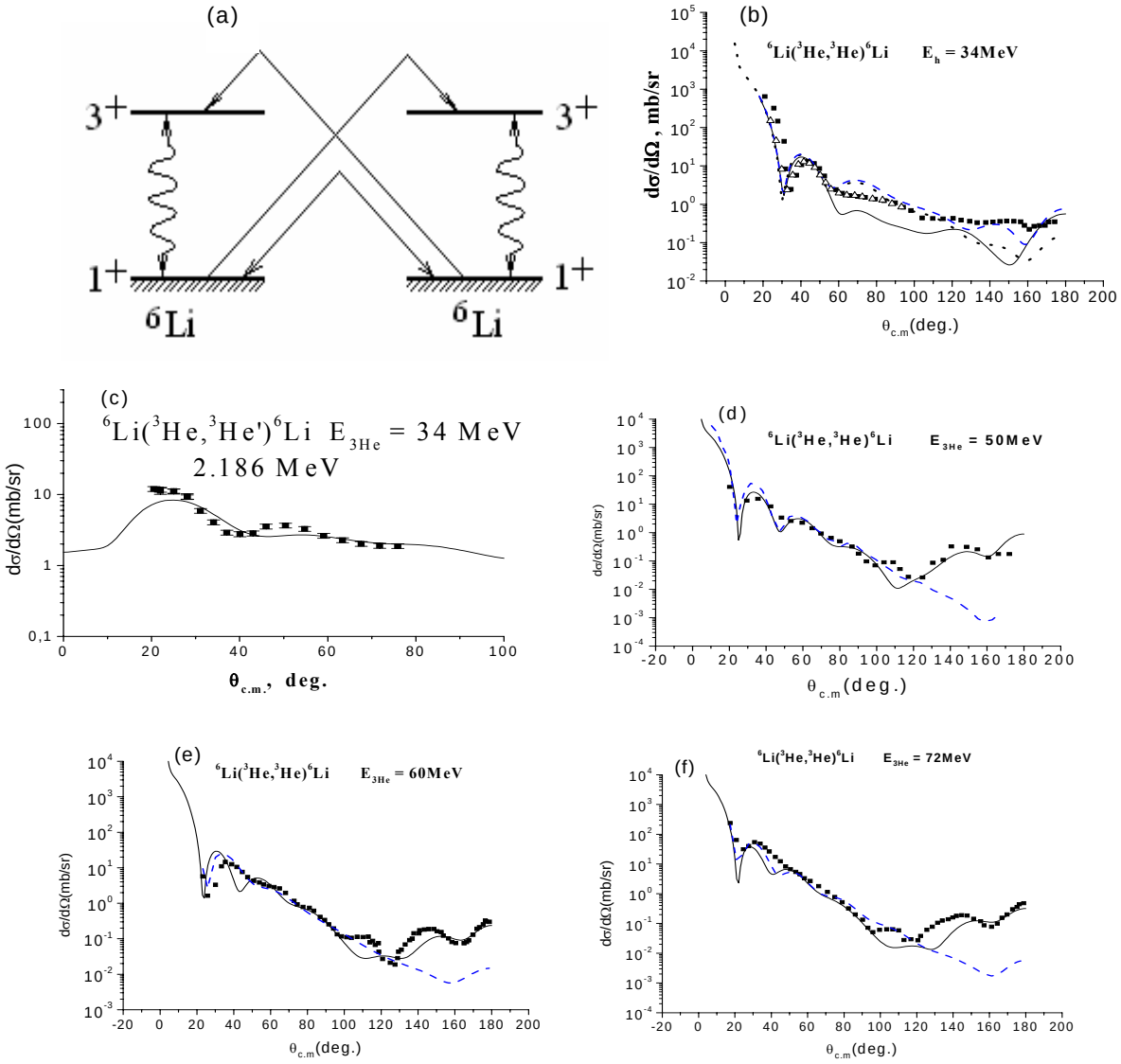

Fig. 4. Comparison between calculated and experimental data. (a) is a coupling scheme used in calculations of inelastic scattering with taking into account the triton cluster exchange. The open up-triangle dots in window (b) and dots in (c) are our measurements of elastic and inelastic (with excitation E*=2.185 MeV, 3+ state) ^{3}He scattering, and the solid squares data in (b) were taken from Chuev et al. [30] dots in (d), (i), (f) are the experimental data taken from [17] for 50, 60, 72 MeV, dash lines are the results of calculation with ordinary OMP with potentials (10-15) from the table 2, and solid lines are CRC calculations for triton transfer with elastic scattering at 34, 50, 60, and 72 MeV. Dot line in window (b) is the OMPs calculation with potential 4(1) from the table 2

c) Evaluation of more complicated mechanisms of the reaction ^{6}Li(^{3}He,*d*)^{7}Be

We use FRESCO code to do the subsequent calculations. The spectroscopic factor deduced in case of the ^{6}Li(^{3}He,*d*)^{7}Be reaction at 34 MeV using Fresco is close to theoretical value if right optical potential parameters used and triton-exchange with elastic and inelastic scattering is involved. Triton transfer has a small effect on the elastic and inelastic scattering, and proton transfer

reaction for ground and first excited state in the reaction ^{6}Li(^{3}He,*d*)^{7}Be. CRC method has been used in our calculations.

Figures 5 and 6 are the differential cross sections of the ^{6}Li(^{3}He,*d*)^{7}Be at $E_{^{3}He}$=33.3 MeV [25] and 34 MeV respectively. CRC predictions of cross sections calculated with potential *1(1)+3(2)* shown in the table 2. In the CRC treatment the optical potential required modifications especially imaginary potential depth, it should be reduced. We had adjusted not only the depth of imaginary part but also other parameters.

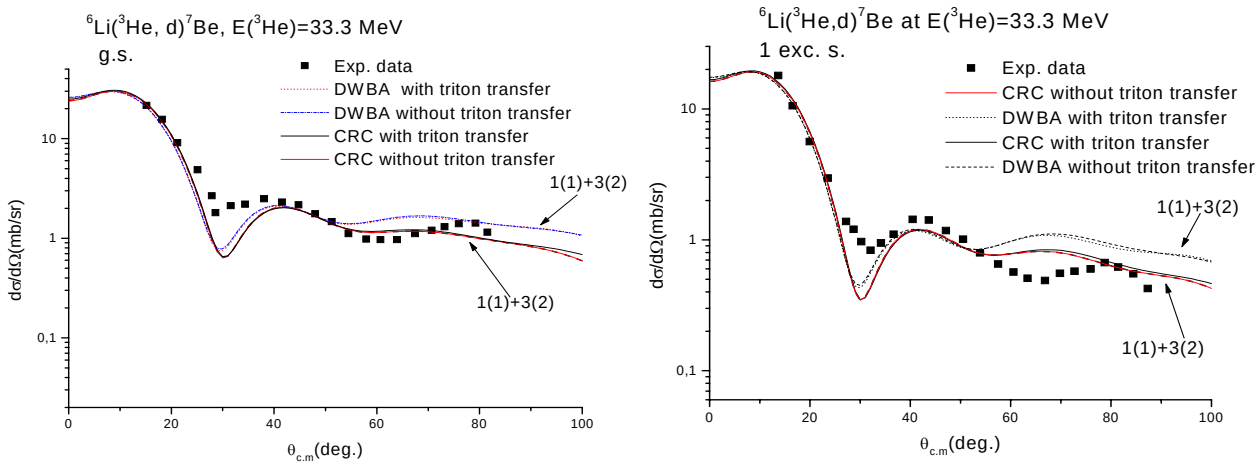

Fig.5. Angular distribution of deuterons from the reaction ^{6}Li(^{3}He,*d*)^{7}Be(g. s, and 1 exc. s.) at $E_{^{3}He}$=33.3 MeV from ref. [25], where Exp. Data (dots). CRC and DWBA predictions of cross sections calculated with potential *1(1)+3(2)* shown in the Table 2. The solid lines represent CRC analysis for the ^{6}Li(^{3}He,*d*)^{7}Be reaction in case of triton transfer with elastic scattering, and inelastic scattering has been involved also. Dot lines are DWBA for ^{6}Li(^{3}He,*d*)^{7}Be reaction with elastic and inelastic scattering without taking into account triton transfer with elastic scattering. Dash lines are DWBA with triton transfer

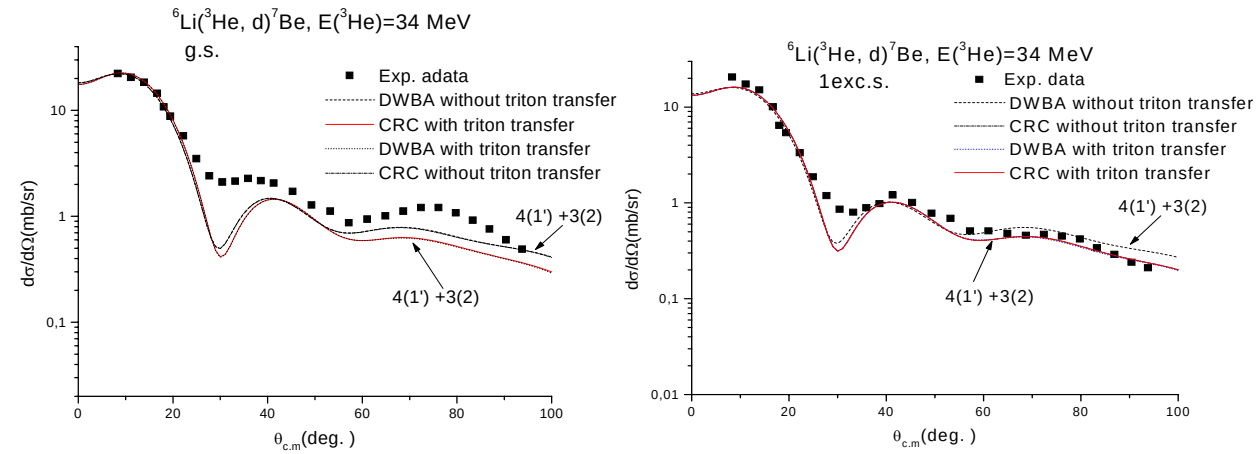

Fig.6. Angular distribution of deuterons from the reaction ^{6}Li(^{3}He,*d*)^{7}Be(g. s, and 1 exc. s.) at $E_{^{3}He}$=34MeV, experimental data (dots). CRC predictions of cross sections calculated with potential *4(1') +3(2)* shown in table 2. The solid lines represent CRC analysis for the ^{6}Li(^{3}He,*d*)^{7}Be reaction in case of triton transfer with elastic scattering, and inelastic scattering. Dash Dot lines are CRC analysis for the ^{6}Li(^{3}He,*d*)^{7}Be reaction without triton transfer with elastic scattering. Dot lines are DWBA for ^{6}Li(^{3}He,*d*)^{7}Be reaction with elastic and inelastic scattering without taking into account triton transfer with elastic scattering. Dash lines are DWBA with triton transfer

We have to say that we start with potential *4(1)*, and the fitting has been made by Fresco program at 34 MeV and we obtained *4(1')* potential parameters which used in our calculations at 34 MeV. The depth of both real and imaginary potentials had increased to achieve the best fit with elastic and transfer reaction as shown in figure 5 and 6. CRC predictions of cross sections calculated with potential *4(1') +3(2)* shown in table 2, the same optical parameters have been used in these analyses to know exactly the effect of triton transfer with elastic scattering on the transfer reaction ^{6}Li(^{3}He, d)^{7}Be in spite of many optical parameters (shown in table 2) could fit the data. As shown in figures 5 and 6 at small angles, small effect appears from the triton transfer with elastic scattering on the ^{6}Li(^{3}He, d)^{7}Be reaction.

Table 3. The values of spectroscopic factors of ^{7}Be extracted from literature

E^* (J^π) MeV	lj	c^2S (FRESCO)		[31]
		E_{3He}=33 MeV [23]	E_{3He}=34 MeV	
0.0 ($3/2^-$)	1/2	0.27±0.027	0.27±0.036	0.29
0.0 ($3/2^-$)	3/2	0.43±0.027	0.31±0.036	0.43
0.429 ($1/2^-$)	1/2	0.03±0.027	0.028±0.036	0.039
0.429 ($1/2^-$)	3/2	0.84±0.027	0.75±0.036	0.85

d) ^{6}Li(p,γ)^{7}Be reaction at the low energies

For each angle the γ-detector was 6 cm from the beam spot on the target. The detector just as the calibration sources was placed to within 1 mm. The calibration source of ^{137}Cs (E_γ = 661.66 keV) was used to construct the dependence on γ-rays registration rate from the source detector distance. It was determined that at a distance of 6 cm the deviation on ±1 mm results in a change of registration rate on 3.2%. So, the overall uncertainty of the absolute γ-detector photo-peak efficiency determination introduced by statistical uncertainty of γ-ray counts determination, dead time of the measuring electronics and inaccuracy of the γ-detector position was adopted 5.5% along the whole range of energies of registered γ-rays. The angular distributions of the ^{6}Li(p,γ)^{7}Be reaction were fitted at four fixed energies from the energy region of $E_{p,\,lab.}$ = 387 - 1283 keV by Legendre polynomials [32]:

$$W(\theta_\gamma) = 1 + \Sigma_k a_k Q_k P_k(\cos\theta) \quad (k = 1,2,\ldots), \tag{6}$$

where a_k are the expansion coefficients and Q_k are the attenuation coefficients, which take into account solid angle subtended by the γ-detector. In view of the limited number of angles, the fits were carried out by including only k = 1 and 2. The lower limits of Q_1 and Q_2 were calculated for the conditions of experiment within the point radioactive source approach by using the known dimensions of sensitive region of the γ-detector, the source-detector distances (D), and without taking lead plate located in front of the γ-detector into account. The lower limits of Q_1 and Q_2 were calculated for the conditions of experiment within the point radioactive source approach by using the known dimensions of sensitive region of the γ-detector, the source-detector distances (D), and without taking lead plate located in front of the γ-detector into account. Q_i can be written:

$$Q_i = \frac{J_i}{J_0} \qquad (i = 1, 2), \tag{7}$$

where $J_k = \sum_{i=0}^{3} \int_{\theta_i}^{\theta_{i+1}} P_k(\cos\alpha) \cdot [1 - e^{-\mu(E_\gamma)\cdot l_{i+1}(\alpha)}] \cdot \sin\alpha \cdot d\alpha$, ($k$ = 0, 1, 2), and $\mu(E_\gamma)$ is absorption coefficient.

Depending on our calculations [13, 14] for ^{6}Li(p, p)^{6}Li, we could calculate enhanced optical potential parameters at low energies. Using spectroscopic factors have been extracted from our

experimental data of the reaction ^{6}Li(^{3}He,d)^{7}Be, we could calculate of the cross section of the ^{6}Li (p,γ)^{7}Be reaction was carried within the framework of the direct capture in the potential model using FRESCO Code. The calculation of the cross sections depended on OMPs from ^{6}Li(p, p)^{6}Li and spectroscopic factors from the reaction ^{6}Li(^{3}He,d)^{7}Be. For us it was cheerful results to obtain the values of cross section directly from our calculations depending on OMPs from the reaction ^{6}Li(p,p)^{6}Li. The relation between spectroscopic factors and optical potential parameters used was verified here very clear. As shown in fig.7, when we used extracted spectroscopic factors from ^{6}Li(^{3}He,d)^{7}Be, we obtained dot line.

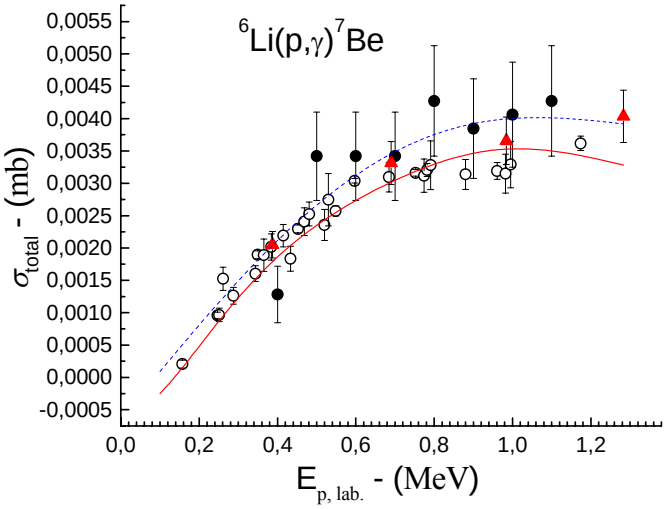

Fig. 7. Total cross section of the reaction ^{6}Li(p,γ)^{7}Be**.** The experimental points are from [8] (open circles), [33] (closed circles) and our measurements as triangle. Solid line is calculated data depending on the OMPs from ^{6}Li(p, p)^{6}Li in ref. [13,14] where dot line represents the calculations in case of OMPs taken from [34]

Another group of spectroscopic factors were extracted with only our OMPs and just changing in the spectroscopic factors to analysis the experimental data and this is shown as *solid line* in fig. 7. The spectroscopic factors of ^{7}Be at these low energies are energy dependent so their values changed with energy especially at very low energies. For example, the spectroscopic factors for ground state extracted were $1P_{3/2}$= 0.207 and $1P_{1/2}$=0.18 and for excited state were $1P_{3/2}$= 0.306 and $1P_{1/2}$= 0.065 at E_p=387 keV. The right values of spectroscopic factors depend on the choice of OMPs used. In order to calculate the astrophysical *S* factor, we employed the standard expression [35]:

$$S(NJ,J_f) = \sigma(NJ,J_f)E_{\mathrm{cm}} \exp\left(\frac{31.335 Z_1 Z_2 \sqrt{\mu}}{\sqrt{E_{\mathrm{cm}}}}\right), \qquad (8)$$

where σ is the total cross section for the radiative capture process (in barn units), $E_{\mathrm{c.m.}}$ is the c.m. energy of particles in the entrance channel (in keV units), μ is the reduced mass of the entrance-channel particles (in atomic mass units), Z are the charges of the particles (in elementary charge units, e) and N stands for E (electric) or M (magnetic) transitions of multipolarity J to the final (J_f) state of the nucleus. The numerical coefficient 31.335 was obtained by the present authors on the basis of modern values of fundamental constants from [36]. We have S(0)=114±5 eV.b as shown in Figure 8.

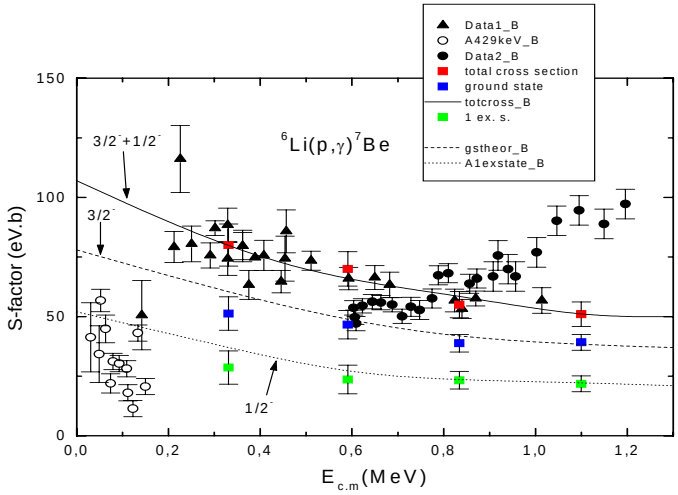

Fig. 8. S-factor calculated using our measurements and Fresco program, the red points are our measurements. The displayed points correspond to experimental data from [8] (they are presented in [10]).

Conclusion

The OMPs have been calculated at low energies for proton elastic scattering on ^{6}Li. New groups of OMPs extracted show linear relation between E_p and V_0. Double folding model could be used to calculate analysis the whole spectrum of ^{3}He scattering on ^{6}Li at 34MeV. Inelastic scattering at E_{3He}=34 MeV has been analyzed where intrinsic quadrupole moment was (-0.818 mb) and $B(E_2)$= 25.6±2.0 e^2 fm^4. The analysis made by us for SFs for ^{6}Li={^{3}He+t}have advantage that the calculations agree well with experimental data. SFs calculated at energies 34, 50, 60, and 72 agree with theoretical values which were 0.58. Value of spectroscopic factor for ^{6}Li={^{3}He+t} reaction is energy dependent where its value at 34MeV is different from the value at 72 MeV. We think that there two parameters have an effect on the extraction of spectroscopic factor: first, the energy of incident particles and second, the OMPs used in extraction. The spectroscopic factor of ^{7}Be={p+^{6}Li }have been extracted from the reaction ^{6}Li(^{3}He,d)^{7}Be and their values agree with theoretical values expected by shell model. The potential model succeeded to calculate the cross section direct capture reaction ^{6}Li (p,γ)^{7}Be at low energies. Astrophysical s-factor calculated in our work is reliable because all values are taken from experimental data measured by us. We have S(0)=114±5 eV.b which gives enhanced value for this important physical factor.

References

1. P. E. Hodgson, the Optical Model of Elastic Scattering (Clarendon, Oxford, 1963).
2. N. Burtbayev, Mrarzhan Nasurralla, Maulan Nasurralla, Zh. K. Kerimkulov, and S. B. Sakuta, American institute of Physics (AIP) Conference Proceeding 2008, 203-208.
3. Ian J. Thompson and Filomena M. Nunes, Nuclear Reactions for Astrophysics: Principles, Calculation and Applications of Low-Energy Reactions(Cambridge, Cambridge University Press, 2009).
4. N. Burtbayev, Mrarzhan Nasurralla, Maulan Nasurralla, Zh. K. Kerimkulov, and S. B. Sakuta, American institute of Physics (AIP) Conference Proceeding 2008, 203-208.
5. S. B. Dubovichenko; N. Burtebaev; D. M. Zazulin ; Zh. K. Kerimkulov; A. S. A. Amar, Physics of Atomic Nuclei, 2011, Volume 74, Number 7, Pages 984-1000.
6. J. T. Huang, C. A. Bertulani, V. Guimaraes, Atomic Data and Nuclear Data Tables 96(2010) 824-847.
7. S. Angulo et al., Nucl. Phys. A 656, 3 (1999).
8. Z. E.Switkowski, J. C. P. Heggie, D. L.Kennedy, D. G.Sargood, F. C.Barker, R. H. Spear, Nucl. Phys. A, Vol.331 (1979) 50-60.

9. F. C. Barker, Aust. J. Phys. 33 (1980) 159.

10. K. Arai, D. Baye, P. Descouvement, Nucl. Phys. A 699 (2002) 963-975.

11. R. M. Prior, M. C. Spraker, A. M. Amthor, K. J. Keeter, S. O. Nelson, A. Sabourov, K. Sabourov, A. Tonchev, M. Ahmed, J. H. Kelley, D. R. Tilley, H. R. Weller, and H. M. Hofmann, physical review C 70, 055801 (2004).

12. F. E. Cecil, D. Ferg, H. Liu, J. C. Scorby, J. A. McNeil, and P.D. Kunz, Nucl. Phys. A539, 75 (1992).

13. S. B. Dubovichinko, N. Burtebayev, D. M. Zazulin, Zh. K. Kerimkulov, A. Amar. Yad. Physika, Vol. 74, No. 7, (2011) 1013-1028.

A. Amar, Sh. Hamada, N. Burtebayev, N. Amangeldy, International Journal of Modern Physics E, Vol. 20, No. 4 (2011) 980–986.

14. Fresco, I. J. Thomson, Department of physics, University of Surrey, Guildford GU2 7XH, England, version FRES 2.0, July 2006.

15. V. N. Bragin, N. T. Burtebaev, A. D. Duisebaev, G. N. Ivanov, S. B. Sakuta, V. I. Chuev, and L. V. Chulkov, Yad. Fiz. 44, (1986) 312.

16. T. Sinha, Subinit Roy, and C. Samanata, Physical Review C, Vol. 47, No. 6 (1993) 2294-2297.

17. P. J. Simmonds, N. M. Clarke, K. I. Pearce, R. J. Griffiths, B. Stanley, S. Roman, A. Farooq, G. Rai, M. C. Mannion, and C. A. Ogilvie, J. Phys. G: Nucl. Part. Phys. 15 (1989) 353-370.

18. J. Cook and R. J. Griffiths, Nucl. Phys. A 366, 27 (1981).

19. L. R. Suelezle, M. R. Yearian, Hall Crannel, Phys. Review vol. 162 No 4(1967) 992.

20. J. Cook , Computer Physics Communications, Vol.25, No 2 (1982)125-139.

21. P.Pereslavtsev et al. Nucl. Instruments and methods in Nuclear Phys. Research B 266 (2008) 3501-3512.

22. C. M. Perey and F. G. Perey, At Data Nucl. Data Tables 17, 1 (1976)

23. A. K. Basak, O. Karban, S. Roman, G.C. Morrison, C.O. Blyth and J. M. Nelson Nuclear physics A368, N1 (1981) 93-107.

24. A. K. Basak, O. Karban, S. Roman, G.C. Morrison, C.O. Blyth and J. M. Nelson Nuclear physics A368, (1981) 74.

25. H. Ludecke, Tan Wan-Tjin, H. Werner and J. Zimmerer. Nuclear Physics, A109 (1968) 676-688.

26. J. R. Patterson, J. M. Poate, B. A. Robson, E. W. Titterton, Proc. Phys. Soc. 90 (1967) 577.

27. D. Y. Pang, R. L. Varner, and R. Wolski, Phys. Rev. C 79, 024615 (2009).

28. D.R. Tilley, C.M. Cheves, J.L. Godwin, G.M. Hale, H.M. Hofmann, J.H. Kelley, C.G. Sheu and H.R. Weller , Nucl. Phys. A708 (2002).

29. V. I. Chuev, V. V. Davidov, B. G. Novatskii, A. A. Ogloblin, S. B. Sakuta, D. N. Stepanov, Journal De Pgysique, Colleque c6, Vol. 32 (1971) 163.

30. S. Cohen and D.Kurath. Nucl. Phys. A101 (1967) 1.

31. J.D. King, R.E. Azuma, J.B. Vise, J. Görres, C. Rolfs, H.P. Trautvetter, A.E. Vlieks, Nucl. Phys. A, Vol.567 (1994) 354-376.

32. R.Ostojic, K.Subotic, B.Stepancic // Nuovo Cim. A76, 1983, P.73-82.

33. B. A. Watson, P. P. Singh, and R. E. Segel, Phys. Rev. Vol. 182, No. 4 (1969) 977-989.

34. W. A. Fowler, G. R. Caughlan, and B. A. Zimmerman, Ann. Rev. Astron. Astrophys. 13, 69 (1975).

35. E. E. Salpeter, Phys. Rev. 88, 547 (1952).

^{6}Li (^{3}He, d)^{7}Be РЕАКЦИЯСЫНЫҢ СПЕКТРОСКОПИЯЛЫҚ ФАКТОРЫ ЖӘНЕ ^{6}Li (p, γ) ^{7}Be РЕАКЦИЯСЫ ҮШІН АСТРОФИЗИКАЛЫҚ ФАКТОР

Н. Бүртебаев, А. Амар, С.Б. Сакута, С.В. Артемов, Ж. Керімкулов

34 МэВ энергияда ^{6}Li ядроларында және ^{6}Li(^{3}He,d)^{7}Be реакциясында ^{3}He ионының серпімді және серпімсіз шашырауының дифференциалдық қимасының бұрыштық үлестірілуі өлшенді. 34, 50, 60 и 72 МэВ энергияларда серпімді шашырау бойынша деректер оптикалық потенциалымен, тритийдің серпімді беріліс механизмін және ^{6}Li спектрскопиялық факторды есепке ала отырып, t+^{3}He сияқты алынған, Fresco программасымен қайта талданды Потенциалдың нақты бөлігінің параметрлері қос үйірткі моделі шеңберінде есептелді. 34 МэВ энергия үшін CRC әдіспен ^{7}Be ядроларының негізгі және бірінші қозбалы күйілеріндегі протонның жұлынып шығу дифференциалдық қимасы талданды. ^{6}Li(^{3}He,d)^{7}Be реакциясында негізгі де және қозбалы күйлер үшін де протонды тасымалдауға тритийдің алмасу механизмінің ықпалы ескеріледі. ^{7}Be ядросы үшін спектрскопиялық факторлар, p^{6}Li конфигурациясы сияқты, эксперименттік деректерден алынды. ^{7}Be ядросындағы негізгі және бірінші қозбалы күйілеріндегі (1/2-, 429 кэВ) γ- өтулері үшін $E_{р,лаб}$= 387, 690, 984 және 1283 кэВ энергияларында ^{6}Li(p,γ)^{7}Be реакциясының бұрыштық үлестірілулері өлшенді. ^{6}Li (p, γ) ^{7}Be реакцияның қимасының есебі Fresco программасын қолданып, потенциалдық моделде тікелей қармау шеңберінде өткізілді. Эксперименттік деректерден ^{7}Be спектрскоптық факторлары мен ^{6}Li + p → ^{7}Be + γ астрофизикалық факторлары алынды.

СПЕКТРОСКОПИЧЕСКИЙ ФАКТОР ИЗ РЕАКЦИИ ^{6}Li (^{3}He, d)^{7}Be И АСТРОФИЗИЧЕСКИЙ ФАКТОР ДЛЯ ^{6}Li (p, γ) ^{7}Be

Н. Буртебаев, А. Амар, С.Б. Сакута, С.В. Артемов, Ж. Керимкулов

Измерены угловые распределения дифференциальных сечений упругого и неупругого рассеяния ионов ^{3}He на ядрах ^{6}Li в реакции ^{6}Li(^{3}He,d)^{7}Be при энергии 34 МэВ. Данные по упругому рассеянию при энергиях 34, 50, 60 и 72 МэВ проанализированы повторно с оптическим потенциалом, учитывающий механизм упругой передачи трития и спектроскопического фактора ^{6}Li, как t+^{3}He, извлеченным с применением программы Fresco. Параметры действительной части потенциала рассчитаны в рамках модели двойной свертки. Дифференциальные сечения срыва протона в основное и первое возбужденное состояния ядра ^{7}Be проанализированы методом CRC для энергии 34 МэВ. Учитывается влияние обменного механизма трития на перенос протона в реакции ^{6}Li(^{3}He,d)^{7}Be, как для основного, так и для возбужденного состояний. Спектроскопический фактор для ядра ^{7}Be, как конфигурации p^{6}Li получен из экспериментальных данных. Измерены угловые распределения реакции ^{6}Li(p,γ)^{7}Be при энергиях $E_{р,лаб}$ = 387, 690, 984 и 1283 кэВ для γ-переходов в основное и первое возбужденное (1/2-, 429 кэВ) состояний в ядре ^{7}Be. Расчеты сечения реакции ^{6}Li(p,γ)^{7}Be проводились в рамках прямого захвата в потенциальной модели с использованием программы Fresco. Из экспериментальных данных извлечены спектроскопические факторы ^{7}Be и астрофизические факторы ^{6}Li + p → ^{7}Be + γ.